Advances in Military Technology
Vol. 21, No. 2, 2026, pp. 413-428
ISSN 1802-2308, eISSN 2533-4123
DOI 10.3849/aimt.02089

Design of a Supervised Autonomous Ground Vehicle for Armored Target Neutralization

K. Abdullayev[1], V. Gasimov[2], F. Dadashov[3], N. Huseynov[3], H. Hesenov[4*], and Z. Mahiyadinov[5]

[1] *Radio-Electronics Department, National Academy of Aviation, Baku, Azerbaijan*
[2] *Faculty of Information and Computer Engineering, Baku Engineering University, Baku, Azerbaijan*
[3] *AI Technologies Department, National Academy of Aviation, Baku, Azerbaijan*
[4] *A Laboratory for Aircraft Development and Design, National Academy of Aviation, Baku, Azerbaijan,*
[5] *SINAM LLC, Baku, Azerbaijan*

The manuscript was received on 4 February 2026 and was accepted after revision for publication as a case study on 1 September 2026.

Abstract:

This paper presents the design and experimental evaluation of an intelligent, supervised semi-autonomous unmanned ground vehicle (UGV) for military target neutralization. The system employs a compact dual-body tracked chassis with ±30° articulation and a 30 kg gross mass to enhance mobility on uneven terrain. An on-board computer processes infrared (IR) imagery for target detection while an autopilot system executes waypoint navigation and low-level motion control. A ground control interface supports map-based mission planning, real-time telemetry and video monitoring and switching between manual and autonomous operation. Upon target detection, the operator is alerted and engagement proceeds only after explicit confirmation thereafter terminal action is safely emulated at close range via a digital trigger. Simulation and field trials indicate stable mobility, reliable waypoint tracking and near-real-time detection performance.

Keywords: *target detection, YOLO, on-board processing, autonomous navigation, UGV*

1 Introduction

UGV systems are increasingly used for tasks that would otherwise place personnel in high-risk situations, such as reconnaissance, route inspection and operations in con-

* *Corresponding author: A Laboratory for Aircraft Development and Design, National Academy of Aviation Institution, Mardakan ave. 30, Baku, Azerbaijan. Phone: +994 507 875 425, E-mail: hesenovhuseyn666@gmail.com. ORCID 0009-0004-7266-0734.*

tested environments [1, 2]. In military applications, compact tracked platforms are particularly attractive because they can traverse uneven terrain, negotiate obstacles and operate in areas where direct human presence is unsafe. These operational demands motivate the development of UGV systems that combine robust mobility, reliable control and mission-oriented payload integration within a compact field-deployable architecture.

Although autonomy has advanced rapidly, fully autonomous lethal decision-making remains controversial and constrained by legal, ethical and operational considerations [3]. For this reason, many practical systems adopt supervised autonomy, where the human operator remains in the loop for safety-critical actions. This human-in-the-loop approach preserves the advantages of autonomous perception and navigation while ensuring that terminal mission decisions remain subject to explicit operator control, thereby improving safety, reliability and operational accountability.

A key requirement in such supervised missions is real-time perception that can provide dependable situational awareness and timely target detection. Deep learning-based detectors, especially the YOLO family, have demonstrated strong real-time performance on embedded platforms [4]. They have also shown promise for IR imagery where visibility may be degraded, and conventional visual sensing becomes less reliable [5]. Therefore, IR sensing combined with lightweight object detection models provides a practical basis for on-board target-alert generation under representative field conditions.

Several UGV platforms have already been developed for reconnaissance, transport, hazardous-field missions but many existing systems are designed as larger multi-purpose solutions rather than compact mission-tailored platforms. The motivation for developing the present vehicle was therefore not the absence of prior UGV technology but the need for a smaller supervised field platform with design features adapted to difficult terrain and extended operation. In this respect, the proposed system differs from many conventional tracked layouts through its dual-body configuration which allows relative motion between the two sections and improves terrain conformity during obstacle negotiation. In addition, the use of gyro-scooter type motor-wheel propulsion contributes to comparatively lower current consumption which supports longer duration operation within the compact platform architecture.

Although previous studies have reported important progress in UGV mobility, autonomous navigation and object detection, these capabilities are often investigated separately rather than within a unified supervised mission system. In particular, comparatively limited attention has been given to compact military style tracked UGV platforms that combine on-board IR-based target detection, waypoint-based semi-autonomous navigation [6], supervised engagement logic and safe terminal-action emulation in a single experimentally validated architecture. In addition, relatively few studies report both simulation-based verification and outdoor field evaluation for such integrated supervised systems. As a result, a practical gap remains between separate studies on mobility, perception and navigation, and deployable supervised UGV platforms intended for close-range target neutralization missions.

This paper addresses that gap by presenting the design and experimental evaluation of an intelligent supervised semi-autonomous UGV for armored target neutralization. The proposed system employs a compact dual-body tracked chassis and integrates on-board IR-based target detection, autopilot-based waypoint navigation [7] and real-time operator supervision through a ground control interface. Unlike concepts based on fully autonomous engagement, the proposed platform follows a human-in-

the-loop operational workflow in which target approach may be performed semi-autonomously while terminal action is permitted only after explicit operator confirmation. For safe development and repeatable testing, terminal action is represented through digital trigger emulation rather than any live hazardous payload. The system is assessed through Gazebo simulations and outdoor field trials, reporting mobility behavior, waypoint tracking performance, telemetry and video responsiveness and practical target-detection performance under representative operating conditions.

The main contributions of this work include the development of a compact dual-body tracked UGV platform designed for supervised close-range target-neutralization missions. The proposed system integrates on-board IR perception with autopilot navigation and an operator-confirmed engagement logic to ensure reliable and controlled mission execution. In addition, the mechanical design of the tracked platform is evaluated through traction-oriented analysis and structural verification to ensure stability and mobility in challenging terrain conditions. Finally, the study presents both simulation and outdoor field test results demonstrating stable platform mobility, reliable waypoint navigation, near-real-time target perception, and effective supervised mission operation.

2 System Overview

2.1 System Architecture and Operational Workflow

Fig. 1 summarizes the overall system architecture which integrates operator supervision, on-board perception and autopilot-based navigation into a supervised semi-autonomous UGV mission workflow. The platform is operated from ground control unit via a joystick-based ground control software (GCS) while a radio frequency link (RF) provides bidirectional telemetry exchange for reliable field deployment.

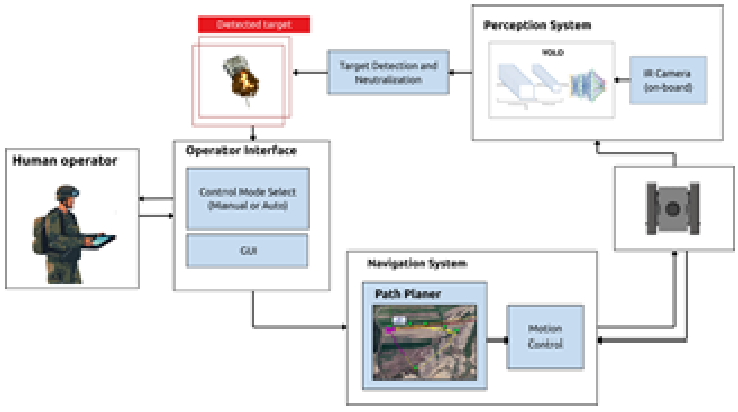


Fig. 1 System level architecture and operational workflow of the supervised UGV

On-board processing is split between an on-board computer and an autopilot-based [8]. The on-board computer captures the IR camera stream and performs YOLO-based target detection while the autopilot executes waypoint navigation and low-level motion control using on-board state estimation (IMU) and the ArduPilot mission engine [9, 10]. The two units communicate over a UART protocol to synchronize operating modes, mission progress and event triggers.

For target search operation, the IR camera is mounted on the front upper section of the vehicle on a gimbal mechanism which provides a practical compromise between forward visibility, mechanical protection and terrain adaptability. During movement, the gimbal-assisted camera scans the surrounding area over an angular sector of approximately 180°, enabling active visual search rather than a strictly fixed forward view. This arrangement improves target observation under uneven terrain conditions, while the dual-body chassis helps preserve useful camera line of sight when pitch changes occur during obstacle negotiation.

The platform supports full manual and semi-autonomous operation as well as return to launch (RTL) and emergency stop (E-stop). In semi-autonomous mode the operator plans a waypoint mission in the map-based GCS and uploads it to the autopilot for execution. During traversal the perception module continuously scans for targets. When a target is detected, the system notifies the operator via a GCS pop-up and offers two options: confirm autonomous engagement or switch to manual control and perform the approach manually.

Engagement follows a supervised sequence with explicit safety constraints. Terminal activation is permitted only after a two-step Yes-No confirmation and only when the vehicle is within 1 m of the target [3]. A timeout and an abort path are provided to cancel engagement when required. For safe development and evaluation, the terminal kamikaze action is emulated by generating a digital trigger status that is reported to the GCS rather than initiating a live explosive event.

2.2 Mechanical Design and Simulation

The UGV adopts a compact tracked design with a dual-body mechanical layout. The right and left modules are connected by an articulated joint that provides approximately ±30° pitch motion allowing the vehicle to conform to uneven ground and maintain track contact during obstacle negotiation [11, 12]. Locomotion is provided by two main tracks left and right enabling differential steering and in-place turning. Fig. 2 shows the complete 3D model of the platform with the principal external dimensions annotated.

The overall dimensions of the platform are 60 cm in length, 60 cm in width and 26.6 cm in height with a ground clearance of approximately 10.5 cm. The total system mass is around 30 kg. The vehicle is designed for high-mobility missions, achieving a maximum speed of up to 8.33 m s^{-1} and a nominal cruise speed of approximately 5.56 m s^{-1}. Propulsion is provided by two brushless (BLDC) motors where each sidetrack is driven by an individual motor through an H-bridge driver configuration. Power is supplied by a battery, selected to support short-duration high-power maneuvers and sustained cruising during waypoint-based missions.

The mechanical structure was modeled as a complete 3D CAD assembly in SolidWorks including the internal volume reserved for the explosive payload (mine) housed within the main body. To verify mechanical robustness under operational loads, a structural stress and deformation analysis was conducted on critical load-bearing components. The analysis confirmed that the resulting deformation remains within acceptable limits for the intended mission profile, supporting the suitability of the chassis for high-mobility operation and terrain-induced loading.

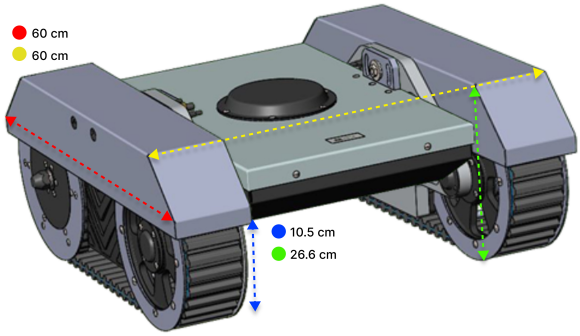


Fig. 2 3D model of the UGV with dimensions

2.3 Tractive Force Estimation and Structural Stress Analysis

To verify the locomotion feasibility of the tracked UGV, the required tractive effort was estimated analytically and supported by SolidWorks-based static and dynamic simulations. The evaluation considered a 30 kg loaded platform operating on grass, field and dry soil including rolling losses, terrain resistance, drivetrain efficiency, slip effects and slope operation up to 25° within the nominal speed range (4–6 m s^{-1}).

The tractive force requirement was computed using a simplified traction balance, where the available drawbar pull must overcome terrain-related resistance and the slope component:

$$F_t \geq mgC_{rr} + mg\sin\theta \tag{1}$$

$$F_{req} = \frac{F_t}{\eta}(1+s) \tag{2}$$

where m is the total mass, g is the gravitational acceleration, Crr is the equivalent rolling-terrain resistance coefficient, θ is the slope angle, η is the drivetrain efficiency and s is the slip coefficient. This formulation provides a conservative estimate for whether the propulsion system can sustain forward motion and manoeuvring under representative field conditions.

In addition to analytical estimation, SolidWorks motion studies were performed to observe platform behavior during obstacle negotiation (stepped and inclined surfaces) and aggressive maneuvers such as in-place turning. A complementary static structural analysis focused on critical load-bearing components, particularly the articulated joint bracket, using an aluminum material model. The simulation results indicated that the induced stresses and deformations remain within acceptable limits for the intended operating profile supporting the mechanical suitability of the proposed design.

2.4 Gazebo Simulation Environment

Gazebo integrated with robot operation system (ROS) Melodic was used to evaluate the developed UGV in a controlled and repeatable virtual testbed [2, 13]. The SolidWorks digital twin was exported as STL (geometry) and URDF (kinematics-physics) and deployed in Gazebo using a dedicated track plugin. As shown in Fig. 3, the UGV navigates toward and engages a simulated main battle tank target.

DOI 10.3849/aimt.02089

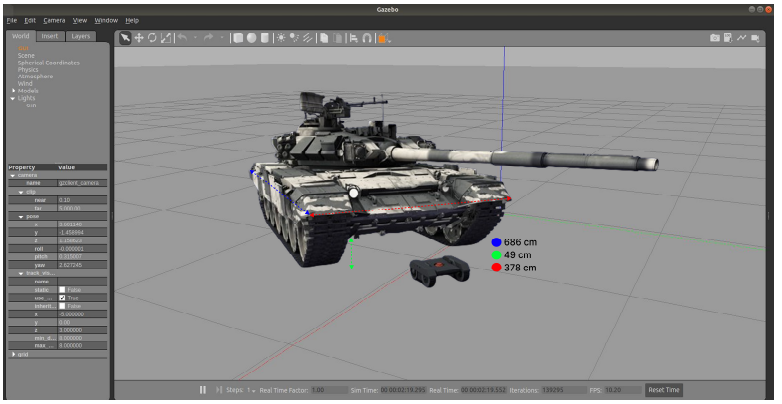


Fig. 3 Autonomous UGV engaging simulated target (Tank) in Gazebo environment

The simulation framework supported parameterized tests with configurable terrain properties, lighting and obstacle placement. An IR camera model and a ROS-based perception node using a YOLO configuration similar (but not identical) to the real system were integrated into benchmark target detection under consistent conditions [2, 5].

The resulting performance metrics are summarized in Tab.Tab. 1, including mobility, detection performance, endurance and the approximate end to end video delay (on the order of 0.2 s). Overall, the Gazebo environment served as a practical verification baseline prior to field experiments.

Tab. 1 Summary of Gazebo-based simulation outcomes

Test scenario	Evaluated metric	Observed value
Linear trajectory traversal	Maximum attainable speed	7.03 m s^{-1}
Ninety-degree rotational maneuver	Minimum turning radius	0.85 m
Target identification and engagement	Frame level detection rate	94.6 %
IR assisted imaging under nocturnal conditions	Effective detection range	35 m
Energy depletion simulation	Endurance duration with nominal load	1 h 30 min
Video telemetry performance	End to end average transmission delay	180 ms

3 Electrical and Control Hardware

The electrical and control architecture of the proposed UGV is designed to support reliable tracked locomotion, autonomous waypoint execution and supervised target engagement under field conditions. The system integrates on-board computing, autopilot-based navigation, propulsion control, perception sensors and a long-range RF communication link. Fig. 4 illustrates the overall hardware interconnection diagram of the platform.

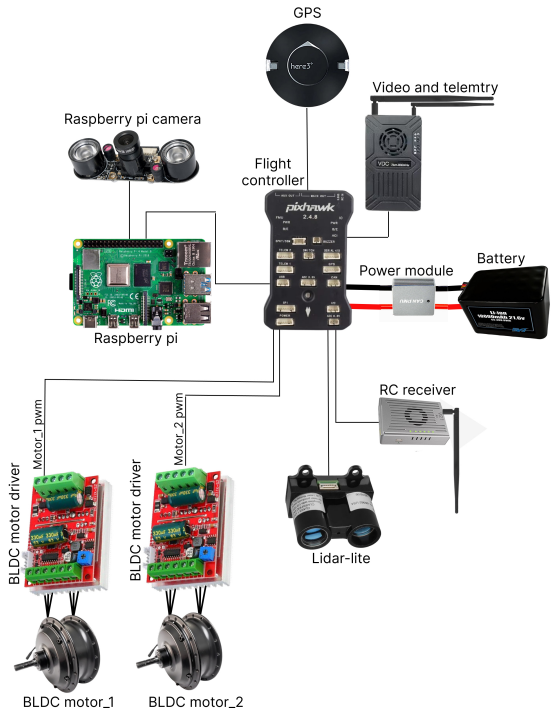


Fig. 4 Modular logical architecture of the electronic control system

At the core of the control stack, an autopilot is responsible for mission execution and low-level motion control via the Ardupilot framework. It provides on-board inertial sensing for state estimation and interfaces with positioning sensors for autonomous navigation [9, 10]. On-board computer serves as the companion computer and runs the perception and decision support processes including IR video acquisition and on-board object detection. On-board computer and autopilot communicate through a UART telemetry interface to exchange mission states, mode commands and event notifications.

For perception and navigation sensing, the platform employs an IR camera mounted on the upper front section of the vehicle on a gimbal for real-time target search, visual feedback and on-board detection. A forward-mounted range sensor with an operating range of approximately 5 cm to 40 m is used for close-range distance estimation during engagement. GNSS is used to support autonomous navigation with the receiver integrated within the vehicle body as part of the on-board navigation stack. Propulsion is achieved using two BLDC motors (left and right tracks) each controlled by a dedicated BLDC motor driver that receives motion commands derived from the autopilot control outputs.

Power distribution is based on a 6-cell lithium polymer battery pack rated at 24 V and 18 000 mAh hour capacity. A main power switch is used for system level power control and a converter 24 to 5 volt supplies regulated power to the on-board computer and low voltage subsystems, ensuring stable operation of computation and sensing during high load maneuvers.

The main electrical and control hardware components used in the developed UGV are summarized in Tab. 2.

Tab. 2 Electrical and control hardware summary of the developed UGV

Component	Key specification
Autopilot	Pixhawk 2.4.8 mission execution
GPS module	GNSS-based localization for autonomous missions
Range sensor	Lidar lite range measurement
Telemetry, video	Telemetry and real-time video to GCS
Camera	IR camera for on-board detection support
Motor and driver	BLDC motors, ZS-X11D driver
Power source	24 V, 18 000 mAh LiPo battery
RC receiver	V21 RC link for manual override

Communication with the ground control station is provided through a long-range RF data link that supports bidirectional telemetry and video streaming for operator supervision. Safety critical operation relies on ArduPilot arming-disarming logic controlled from the interface when disarmed motion commands are blocked and the motors remain inactive. An E-stop is also available in the GCS to immediately halt the vehicle. For simulation and safe field testing, terminal activation is emulated using an on-board computer GPIO trigger: a digital "true" status is generated and reported to the GCS to confirm the engagement event rather than initiating any real explosive mechanism.

4 Ground Control Interface and Autonomous Navigation System

4.1 Mission Software Architecture

The mission software is written in Python programming language and runs on the on-board computer based Raspbian operation system providing a single integrated interface for perception, mission planning and supervised navigation [8]. As shown in Fig. 5, the GCS interface combines a real-time video window, a map-based mission planner, mode buttons, manual driving controls and a live telemetry dashboard, along with simple orientation widgets (gyroscope and compass).

Internally, the software runs in a simple main loop and uses several background threads, so the interface stays responsive while data keeps coming in. One thread handles telemetry and mission control allowing the operator to switch modes, upload waypoint missions to the autopilot and update the telemetry panel in real time. A separate thread receives the RTSP video stream and displays it in the GCS interface therefore when the YOLO detector finds a target the system marks it with a red bounding box on the video. At the same time a logging thread saves mission and system data to CSV files including mission status, telemetry samples, detection events and trigger timestamps.

Mission planning is performed directly on the embedded map. The operator creates waypoints by clicking on the map and a context menu provides actions such as

"move to here", "move to coordinate" and set speed. Planned missions can be saved, started and updated during execution with support for speed and waypoint updates as well as pause and resume control. The planned route is visualized on the map to maintain situational awareness during autonomous operation.

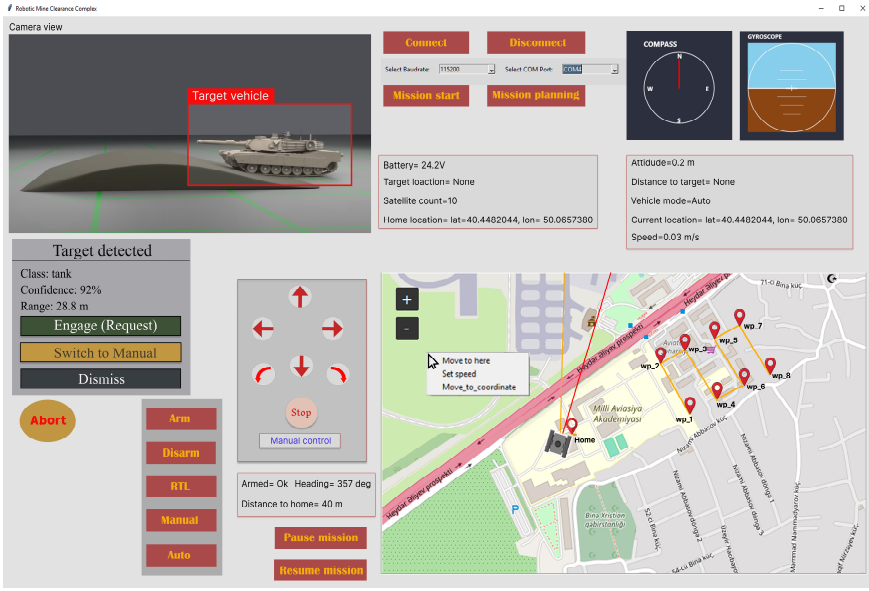


Fig. 5 Ground control interface for mission planning and real-time monitoring

The interface supports Manual, Auto and RTL modes. Manual control is provided through directional buttons for forward, backward, left, right and in-place rotations. For supervised engagement the operator confirmation workflow is managed by an engagement manager which implements the two-step confirmation logic and reports the final terminal action through a True-False status indicator. Fail-safe behaviors are also integrated: an operator triggered E-stop halts the system while RTL is activated automatically if battery level drops below 20 % or if a link-loss condition persists for more than five minutes.

4.2 Autonomous Operation and Target Engagement

Autonomous operation is initiated by the operator through the mission start control in the GCS interface. Before execution, the operator defines the mission region on the map as a polygon and generates the waypoint set within this area [6]. The system enforces a high initial power requirement and allows mission start only when the battery level is at least 95 % while a low-battery threshold of 20 % triggers an automatic return to home action. The overall mission sequence and decision logic are summarized in the algorithmic flowchart shown in Fig. .

In autonomous mode the UGV follows the uploaded waypoints one by one, and the operator can adjust waypoints or speed during the mission if needed. At the same time, the on-board perception module continuously analyzes the IR camera feed using a YOLO-based detector. If no target is found, the vehicle simply keeps tracking the planned route. When a target appears in the camera view, the system shows a pop-up

DOI 10.3849/aimt.02089

alert in the GCS interface, and the operator chooses either to approve autonomous engagement or switch to manual control and perform the approach manually.

After the operator confirms engagement the UGV stops following the waypoint route and switches to a direct target-approach mode. The waypoint mission is paused and the vehicle moves toward the detected target while trying to keep it near the center of the camera view which helps with short range alignment [14]. The GCS also provides an abort option to cancel the kamikaze sequence that mean if the operator activates it the UGV stops and disengages from the target approach.

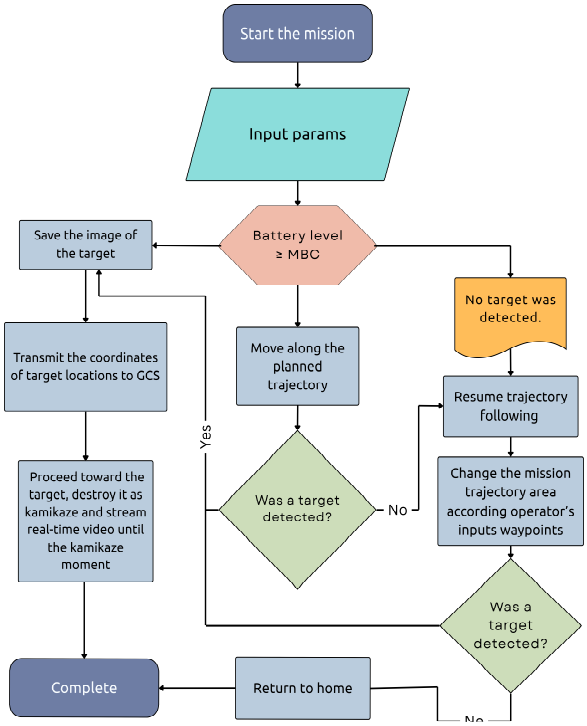


Fig. 6 Autonomous mission and engagement flowchart

Terminal activation is allowed only when the estimated distance to the target drops below 1 m. This close-range check is performed using range sensor measurements together with a vision-based distance estimate. For safe development and testing, the terminal action is not executed physically instead once the condition is met, on-board computer's outputs a digital GPIO "true" signal and the GCS displays it as a trigger status indicator rather than initiating any real explosive event.

Fail-safe behavior is built into the mission workflow. The system automatically switches to RTL if the battery level falls below 20 % or if the communication link is lost for more than five minutes and the operator can also trigger RTL manually from the interface at any time. If the mission finishes without an engagement, the route is marked as completed and the vehicle returns to the home position.

The on-board perception module detects targets in real time using a YOLOv5 model deployed on the companion computer [4]. In our implementation we used that with an input size of 1 024 × 1 024 p, custom anchors and augmentation settings tuned for IR imagery. The model runs CPU only on an on-board computer and processes the

camera stream at 30 fps with inference performed on every frame. Visual data are captured using an "Arducam day-night vision for raspberry pi" with automatic IR cut switching.

A custom dataset was collected and annotated specifically for this platform. It contains 1 400 images and includes a single class represented in practice by a tank target. Labels were prepared in COCO json format and split into train, validation, test sets using a 70 %, 20 %, 10 % random split. During training we applied data augmentation tuned for field conditions including horizontal flip (0.5), scaling (0.5), translation (0.1), mosaic (0.25), HSV value jitter (0.05), blur (0.08) and noise (0.04) while other augmentations were disabled. The model was trained using stochastic gradient descent with a learning rate of 0.01, momentum of 0.937, and weight decay of 0.0005. A warm-up stage was applied during the first three epochs with a lower learning rate of 0.001. The training lasted 200 epochs with a batch size of 8.

Model training was carried out offline on a GPU workstation with 16 GB of VRAM, whereas deployment inference was performed CPU-only on the on-board computer. In addition to the operational field detection rate, standard object-detection metrics were computed on the held-out test set in order to provide an accepted quantitative evaluation of detector performance. On the test dataset, the trained YOLOv5 model achieved a precision of 0.89, recall of 0.85, mAP@0.5 of 0.90 and mAP@0.5:0.95 of 0.61. These values indicate that the detector achieved reliable target localization and classification performance on the annotated IR dataset despite the relatively limited dataset size and the single-class mission specific setting.

In the present implementation, target perception is based on frame-by-frame YOLO detections without an additional temporal tracking layer. This design was selected to keep the on-board perception pipeline computationally lightweight and compatible with CPU-only inference on the companion computer. However, incorporating a tracking stage in future work could further improve temporal stability by maintaining target continuity across consecutive frames, reducing intermittent detection flicker and helping preserve target state during short partial occlusions or brief confidence drops. Such a tracking-assisted perception pipeline would also provide a more stable basis for supervised engagement decisions by introducing temporal consistency in addition to single-frame detector confidence.

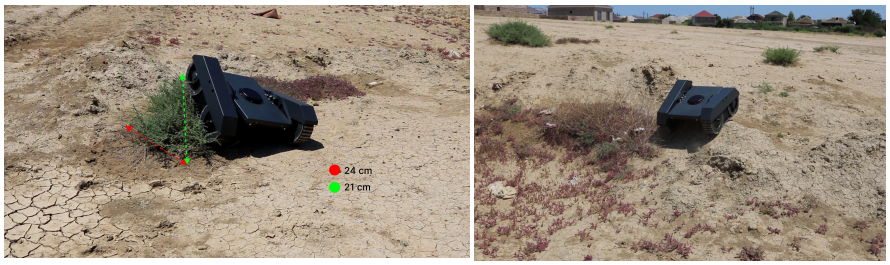
For field trials, performance was additionally reported using a practical frame-level detection rate, defined as the percentage of frames in which the target was detected when it was present in the camera field of view. Using this operational measure, the detection rate in outdoor experiments was approximately 85–90 %. Unlike the test-set metrics, this field measure characterizes real mission behavior under communication, motion and environmental effects rather than benchmark dataset performance alone [15]. Detection latency is defined as the time from camera acquisition to detection and typically ranges from 40 ms to 60 ms, including acquisition, preprocessing, inference and postprocessing.

5 Experimental Setup and Results

5.1 Experimental Setup

Field experiments were conducted in an outdoor environment to evaluate mobility, autonomous navigation and supervised target engagement of the developed UGV. Tests were performed across heterogeneous surfaces representative of real deployment

conditions, including grass-field, dry soil, sand and rocky terrain [11, 16]. The UGV configuration was kept constant throughout all trials with a gross mass of 30 kg and each mission was initiated only after confirming a fully charged battery state that satisfied the mission start threshold (≥ 95 %). Representative mobility trials and size of grass that it passes over are shown in Fig. 6(a) and Fig. 6(b).



(a) *(b)*

Fig. 6(a) UGV traversing dry, cracked terrain while successfully overcoming low vegetation. (b) UGV successfully climbing an uneven mound during mobility test

Three experimental scenarios (S) were executed. S1 evaluated waypoint tracking on a predominantly flat route. S2 assessed target detection and supervised engagement during autonomous traversal where the operator primarily performed confirmation-abort actions through the joystick-driven GCS and occasionally switched to manual driving when required by the environment. S3 examined slope climbing capability on a soil surface with an approximately 25° incline. In S1 and S2, the robot operated for about 20 minutes per run and traversed an approximate route length of 5 km, while S3 focused specifically on the uphill traversal task.

Latency was measured in both Gazebo simulations and outdoor trials using on-board computer software timestamps and a video timestamp overlay. Detection latency was defined as end to end on-board processing time on the on-board computer, measured in Python with *time.time*() function from frame acquisition-preprocessing through YOLO inference and post-processing to the final detection output, yielding (40-60) ms. Telemetry latency was estimated as one-way telemetry delay (on-board computer to GCS) using per-packet send-time (on-board computer) and receive-time (GCS), typically (20–50) ms. Video latency was estimated by rendering a time of capture overlay on frames on the on-board computer before H.264 encoding and comparing the embedded overlay time with the GCS render time therefore the resulting end to end delay was (180–200) ms (capture to encode to RF link to decode to GUI). This approach provides a repeatable operational estimate without requiring cross-device clock synchronization.

All on-board sensing and communication modules were enabled during the experiments, including the IR camera for perception, GPS for localization and a range sensor for proximity assessment. System data were recorded using CSV logging, capturing real-time telemetry (e.g., navigation state, motion-related variables, battery status and GPS position), detection events and terminal trigger timestamps. For safety, explosive activation was not used; instead, the terminal action was emulated by issuing a digital trigger flag from the on-board computer and displaying the corresponding status in the GCS interface.

The outdoor test area included visually heterogeneous background conditions typical of open-field operation, including dry soil, grass, stones and low vegetation around the artificial target location. Although the trials were conducted within a limited mission radius and under a single general weather condition, they still provided a practical environment for observing detector behavior in the presence of background clutter and partial target occlusion.

Acceptable target search conditions were ensured when a practical line of sight existed between the camera and the target region. The front upper camera placement, gimbal stabilization and dual-body chassis reduced view loss under moderate terrain unevenness. The test area contained medium height vegetation and open-field clutter and representative vegetation together with the approximate grass height are shown in Fig. 6(a). Thus, partial target visibility was often sufficient for detection, whereas fully obstructed targets were outside the effective search condition. When taller vegetation interfered with approach, the range sensor supported partial trajectory adjustment.

5.2 Results and Discussion

Overall, the field tests confirmed stable mobility and mission execution across mixed terrains. The UGV demonstrated robust short-range obstacle negotiation during mobility trials, including successful traversal of dry, cracked terrain with low vegetation and climbing over uneven mounds. The quantitative mobility limits obtained from practical trials are summarized in Tab. 3.

Tab. 3 Ability to overcome obstacles

Parameter	Value
Grass height	0.21 m
Embankments	0.15 m
Slopes	25°
Rocky surfaces	0.2 m
Step height	0.2 m

The platform was able to traverse grass height up to 0.21 m, overcome embankments up to 0.15 m, handle rocky surface irregularities up to 0.2 m and negotiate step heights up to 0.2 m while sustaining slopes up to 25° under moderate-speed manual operation.

For autonomous navigation, waypoint tracking accuracy remained within (1–2) m on average with a maximum deviation of approximately 3 m under field conditions. These deviations are consistent with outdoor GPS-based localization and terrain-induced slip effects [9, 10]. The supervised engagement pipeline achieved a field detection accuracy of approximately (85–90) % while simulation results reported higher classification performance (94.6 %) under controlled conditions [13]. In real operation, detection latency remained near real-time, typically within (40–60) ms, supporting timely operator alerts and decision-making.

In addition to the reported detection-rate results, qualitative observations during field trials showed that the perception module remained functional in visually cluttered open-field backgrounds containing soil, grass, stones and low vegetation around the target region. Since the detector was trained primarily on the geometric appearance of the target class, moderate background clutter did not cause critical degradation in

recognition under the tested conditions. Partial occlusion led to a limited reduction in detection performance, estimated at approximately 8 % in difficult views but the target could still often be recognized when a visible portion remained within the camera frame. The use of an IR capable day-night camera also helped maintain practical detector operation under non-uniform outdoor lighting, although these effects were not evaluated through a dedicated multi-condition illumination study. In ambiguous scenes, including cases with vehicle-like visual structures in the background, the supervised human-in-the-loop workflow provided an additional safeguard, since final engagement decisions always remained subject to operator confirmation rather than detector output alone.

Communication performance remained suitable for operator supervision. Telemetry delay was typically within (20–50) ms and end to end video transmission delay was approximately (180–200) ms which maintained effective situational awareness for confirmation and abort decisions. Regarding energy consumption, each ≈ 20 minutes mission consumed roughly (30–40) % of the battery capacity, indicating that repeated short missions are feasible within a single charge cycle depending on terrain and maneuver intensity.

The experiments also indicated several conditions under which system performance may degrade or mission reliability may be reduced. From the perception perspective, detection performance decreased when the target was located beyond approximately 200 m, when the target appeared too close to the camera to be properly framed, or when the observed target appearance differed significantly from the training dataset. Short-term image instability may also occur under vehicle vibration, although this effect was mitigated in the developed platform through the use of a gimbal stabilizer. In addition, intermittent detection flicker may appear in difficult views, particularly during rapid relative motion or less favorable target presentation.

From the navigation and mission-execution perspective, reliability may be degraded by GNSS inaccuracy, waypoint deviation and operation in environments affected by jammer systems, where localization and route following performance can be reduced. Such deviations become more critical if the platform moves beyond the effective operating range of the telemetry link since loss of communication may then limit operator supervision. Communication performance may also degrade under RF-link weakening or telemetry packet loss. Mechanically, the tracked platform maintained satisfactory mobility within the tested envelope but performance is expected to decrease on rough terrain at higher speeds and on slopes steeper than approximately 25°. Finally, the close-range engagement logic may be affected if the 1 m terminal threshold is estimated inaccurately which can influence the stability of the final engagement decision. These observations define the current operational limits of the proposed system and motivate future improvements in perception robustness, localization resilience and terminal-decision stability.

During field operation, occasional frame-level flickering detections were observed in difficult views, especially when target presentation changed rapidly or visibility became less favorable. Although these events did not directly lead to unsafe autonomous terminal behavior because final engagement always required explicit operator confirmation, they may reduce perception stability and operator confidence during approach. A target-tracking module could mitigate this limitation by smoothing short-term detector fluctuations, maintaining a persistent target hypothesis across frames and reducing the impact of brief missed detections. Therefore, integrating a lightweight tracking approach represents a practical next step for improving percep-

tion robustness and supporting more reliable engagement decisions in supervised mission scenarios.

Finally, terminal activation was tested in a safe and repeatable way using an emulation procedure. Engagement was allowed only after the vehicle reached close range (distance < 1 m), estimated using the range sensor and supported by an optical distance approximation. Once this condition was met, the on-board system produced a digital GPIO "true" trigger which was logged and shown in the ground control interface. This allowed the full supervised engagement sequence to be verified without using any hazardous payload.

Compared with general-purpose tracked UGVs, the proposed system offers compact size, dual-body terrain conformity, on-board IR perception and real-time operator supervision. Its main limitations are the single-class detector, GNSS dependence, jammer sensitivity, limited sensor fusion and the payload, speed and range constraints of a compact platform.

6 Conclusion

This paper presented the design and implementation of an intelligent supervised semi-autonomous unmanned ground vehicle for armored target neutralization. The system combines a compact tracked platform with a modular architecture: on-board perception supports operator-supervised engagement while an autopilot system handles waypoint navigation and low-level motion control. A ground control interface provides mission planning, live telemetry and video monitoring and smooth switching between manual and autonomous modes. For safe testing, terminal activation was verified using a digital trigger emulation rather than a live explosive payload. Structural verification, traction-oriented analysis and Gazebo simulations were used to assess feasibility and outdoor field experiments on mixed terrain confirmed reliable mobility, practical obstacle limits and near-real-time detection behavior under representative conditions. Future work will focus on improving robustness in cluttered scenes, incorporating temporal target-tracking methods to reduce flickering detections and improve engagement stability, and extending target prioritization and terrain-aware navigation to increase operational reliability [14, 16, 17].

References

[1] BUŻANTOWICZ, W. and P.B. TUREK. Autonomous Combat Support Vehicles in Urban Operations: Tactical and Technical Determinants. *Advances in Military Technology*, 2020, **15**(1), pp. 97-114. DOI 10.3849/aimt.01350.

[2] RAVEENDRAN, R., S. ARIRAM, A. TIKANMAKI and J. RONING. Development of Task-Oriented ROS-Based Autonomous UGV with 3D Object Detection. *International Conference on Real-Time Computing and Robotics*, 2020, pp. 427-432. DOI 10.1109/RCAR49640.2020.9303034.

[3] SEHRAWAT, V. Autonomous Weapon System: Law of Armed Conflict (LOAC) and Other Legal Challenges. *Computer Law & Security Review*, 2017, **33**(1), pp. 38-56. DOI 10.1016/j.clsr.2016.11.001.

[4] REDMON, J., S. DIVVALA, R. GIRSHICK and A. FARHADI. You Only Look Once: Unified, Real-Time Object Detection. In: *Conference on Computer Vision and Pattern Recognition*, 2016, pp. 779-788. DOI 10.1109/CVPR.2016.91.

[5] JIANG, C., et al. Object Detection from UAV Thermal Infrared Images and Videos Using YOLO Models. *International Journal of Applied Earth Observation and Geoinformation*, 2022, **112**, 102912. DOI 10.1016/j.jag.2022.102912.

[6] ZHOU, X., X. YU, Y. ZHANG, Y. LUO and X. PENG. Trajectory Planning and Tracking Strategy Applied to an Unmanned Ground Vehicle in the Presence of Obstacles. *IEEE Transactions on Automation Science and Engineering*, 2021, **18**(4), pp. 1575-1589. DOI 10.1109/TASE.2020.3010887.

[7] MAGID, E., R. LAVRENOV and I. AFANASYEV. Voronoi-Based Trajectory Optimization for UGV Path Planning. *International Conference on Mechanical, System and Control Engineering*, 2017, pp. 383-387. DOI 10.1109/ICMSC.2017.7959506.

[8] ANTONELLI, G., K. BAIZID, F. CACCAVALE, G. GIGLIO and F. PIERRI. CAVIS: a Control Software Architecture for Cooperative Multi-Unmanned Aerial Vehicle-Manipulator Systems. *IFAC Proceedings Volumes*, 2014, **47**(3), pp. 1108-1113. DOI 10.3182/20140824-6-ZA-1003.02366.

[9] VELASKAR, P., A. VARGAS-CLARA, O. JAMEEL and S. REDKAR. Guided Navigation Control of an Unmanned Ground Vehicle Using Global Positioning Systems and Inertial Navigation Systems. *International Journal of Electrical and Computer Engineering,* 2014, **4**(3), pp. 329-342. DOI 10.11591/ijece.v4i3.5183.

[10] CAO, H., et al. Autonomous Navigation of Unmanned Ground Vehicles Based on Micro-Shell Resonator Gyroscope Rotary INS Aided by LDV. *Drones*, 2025, **9**(10), 706. DOI 10.3390/drones9100706.

[11] BEYCIMEN, S., D. IGNATYEV and A. ZOLOTAS. A Comprehensive Survey of Unmanned Ground Vehicle Terrain Traversability for Unstructured Environments and Sensor Technology Insights. *Engineering Science and Technology, an International Journal*, 2023, **47**, 101457. DOI 10.1016/j.jestch.2023.101457.

[12] ŠVÁSTA, A. and J. FURCH. Evaluation of Existing Unmanned Ground Vehicles Construction and Basic Preconditions for Their Design. *Advances in Military Technology*, 2023, **18**(1), pp. 151-168. DOI 10.3849/aimt.01723.

[13] SÁNCHEZ, M., J. MORALES, J.L. MARTÍNEZ, J.J. FERNÁNDEZ-LOZANO and A. GARCÍA-CEREZO. Automatically Annotated Dataset of a Ground Mobile Robot in Natural Environments via Gazebo Simulations. *Sensors*, 2022, **22**(15), 5599. DOI 10.3390/s22155599.

[14] NOWAKOWSKI, M. Autonomous Navigation for Unmanned Ground Vehicles in Unstructured Terrain. *Studia Informatica, Systems and Information Technology*, 2025, **31**(2), pp. 117-121. DOI 10.34739/si.2024.31.09.

[15] LIU, Q., Z. LI, S. YUAN, Y. ZHU and X. LI. Review on Vehicle Detection Technology for Unmanned Ground Vehicles. *Sensors*, 2021, **21**(4), 1354. DOI 10.3390/s21041354.

[16] SI, J., et al. Trajectory-Prediction-Based Dynamic Tracking of a UGV to a Moving Target under Multi-Disturbed Conditions. *International Conference on Robotics and Automation*, 2024, pp. 18265-18271. DOI 10.1109/ICRA57147.2024.10611690.

[17] XIE, S., R. SONG, Y. ZHAO, X. HUANG, Y. LI and W. ZHANG. Circular Accessible Depth: A Robust Traversability Representation for UGV Navigation. *IEEE Transactions on Robotics*, 2023, **39**(6), pp. 4875-4891. DOI 10.1109/TRO.2023.3308780.